Vision-Based Robust Position Estimation in Probe-and-Drogue Autonomous Aerial Refueling

Gao Yan, Dai Xunhua, Quan Quan

Abstract—**Probe-and-drogue refueling is widely used owing to its simple requirement for refueling equipment and flexibility. For autonomous aerial refueling, determining the distance between an unmanned receiver aircraft and a tanker aircraft is of great importance. In this paper, a vision-based method is proposed to estimate the position of the drogue by using a camera. This method is a two-step process. The first step is to detect the markers fixed on the drogue and match them as a circle. The second step is to improve the image robustness. In addition, the proposed method is verified in the simulation with a virtual reality toolbox. Simulation results indicate that the proposed method can track the circle steadily and estimate its position in real time.**

I. Introduction

Aerial refueling is an effective way to increase the range and endurance of Unmanned Aerial Vehicles (UAVs). Some modern aircraft even have the ability to maintain their flight for weeks. Currently, there are two major aerial refueling methods in operation. One is Boom-Receptacle Refueling system (BRR), and the other is Probe-and-Drogue Refueling system (PDR) [1]. The latter is more suitable for UAVs because of its simple requirement of refueling equipment and flexibility, which can work well at various refueling speeds and for multiple receiver aircrafts at the same time [2]. Along with the development of the UAV technology, Autonomous Aerial Refueling (AAR) systems are urgently needed. However, the probe-and-drogue system has an apparent drawback, which is susceptible to disturbances, making docking very difficult [3]. Thus, the autonomous aerial refueling requires precise relative position between the receiver aircraft and the drogue of the refueling system [4].

During the past decades, researchers have been making significant efforts to design position estimation methods, including Inertial Measurement Unit (IMU), Global Positioning System (GPS) [5], and vision-based position method [6]. One aspect to note is that due to the restriction of the safety, it is not permitted to attach electronic devices onto the drogue. Relative position information can be obtained from IMU measurements, but zero drift and accumulative error result in its accuracy not meeting the requirements. GPS method has been made in 5cm to 10cm accuracy for formation flying, but problems emerge with accuracy decreasing because of signal blocked or other interference factors. In addition, it is hard to attach the GPS equipment to the drogue. Thus, as a newly-developed contactless method, the vision-based position sensor like a camera is a preferable solution to get the relative position [7].

The research on vision-based position estimation has been developing in the world, and many meaningful achievements have been made [8][9][10]. The existing schemes of vision-based refueling system can be classified into two groups: image based algorithm and feature tracking algorithm. The image based algorithm regards the visual sensor as a two-dimensional sensor, whose characteristics such as image Jacobian matrix and gray value can be integrated into the control law. A typical example of this kind of method is the algorithm using the predictive image for vision aids [9]. The feature tracking algorithm implies to obtain the relative position by means of acquiring and tracking specific features (points, lines, etc.) from a visual sensor. The typical examples of this kind of method include a visual positioning system based on infrared vision sensor [11] and VisNAV active vision navigation system [12][13].

In this paper, the main algorithm is a kind of feature tracking algorithm. For example, in VisNAV system, the position and attitude information is obtained by LHM [14] algorithm which is based on a monocular camera and some infrared Light Emitting Diode (LED) marking points. Nevertheless, the LHM algorithm is an iterative algorithm, which is somewhat time-consuming. In face of such a situation, in this paper, a simpler feature point detecting and matching method with relatively high efficiency and reliability is proposed. In addition, some extra measures are taken to improve the robustness of the system.

The main features of this paper are as follows.

1) A feature point algorithm of detecting and matching the markers as a circle is proposed.
2) In order to improve the robustness of the system, a Kalman filter (KF) based method to reduce observation errors is proposed. In addition, several general correspondence methods are proposed to reduce the influence of noise, redundant and losing points.
3) Simulations are carried out to validate the effectiveness of the proposed methods.

This paper is organized as follows. Some preliminaries and problem formulation are introduced in Section II. In Section III, the main algorithm used in this paper is presented. Then, in Section IV, the details and results of the simulation are expressed. Finally, in Section V, the conclusions are presented.

Gao Yan is with School of Automation Science and Electrical Engineering, Beihang University, Beijing 100191, China (email: buaa_gaoyan@buaa.edu.cn)

Dai Xunhua is with School of Automation Science and Electrical Engineering, Beihang University, Beijing 100191, China (email: dai@buaa.edu.cn)

Quan Quan is associate professor of School of Automation Science and Electrical Engineering, Beihang University, Beijing 100191, China (email: qq_buaa@buaa.edu.cn)

II. Preliminaries and Problem Formulation

A. The Layout of Markers

In order to determine the distance among the receiver aircraft, the tanker aircraft and the drogue of refueling system, it is necessary to place some markers on the surface of the latter two. Moreover, in order to represent the geometric characteristics of the drogue, the markers (see Fig. 1) can be distributed on the circle of the drogue canopy with different intervals between them. Combined with physical and algorithmic filtering methods, markers can be easily extracted from the image.

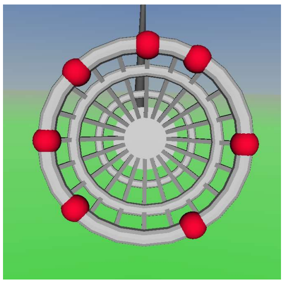

Figure 1. Markers located on the drogue

B. Coordinate System Transformation

In this paper, the coordinate systems are defined as follows (see Fig. 2). The camera coordinate system $o_c - x_c y_c z_c$, is attached to the camera. Its origin is the optical center of the camera, with x_c axis pointing forward, y_c axis pointing right, z_c axis pointing downward. The other system is the drogue coordinate system $o_d - x_d y_d z_d$, whose origin is the center of the drogue. Moreover, its orientation is the same as the camera coordinate system.

Assume that vector $\mathbf{p}_c \triangleq [x_c \; y_c \; z_c]^T$ and $\mathbf{p}_d \triangleq [x_d \; y_d \; z_d]^T$ are in two coordinate systems above. They satisfy [15]:

$$\mathbf{p}_c = \mathbf{R}_d^c \mathbf{p}_d + \mathbf{t}_d^c \quad (1)$$

where $\mathbf{R}_d^c \in \mathbf{R}^{3\times3}$ is the rotation matrix, and $\mathbf{t}_d^c \in \mathbf{R}^3$ is the translation vector. The rotation matrix $\mathbf{R}_d^c$ from the drogue coordinate system to the camera coordinate system can be shown as

$$\mathbf{R}_d^c = \mathbf{R}_z^T(\psi)\mathbf{R}_y^T(\theta)\mathbf{R}_x^T(\phi). \quad (2)$$

In the equation above, with three principal axes, a rotation of angle ϕ about the x-axis is defined as

$$\mathbf{R}_x(\phi) \triangleq \begin{bmatrix} 1 & 0 & 0 \\ 0 & \cos\phi & \sin\phi \\ 0 & -\sin\phi & \cos\phi \end{bmatrix}. \quad (3)$$

Similarly, a rotation of angle θ about the y-axis is defined as

$$\mathbf{R}_y(\theta) \triangleq \begin{bmatrix} \cos\theta & 0 & -\sin\theta \\ 0 & 1 & 0 \\ \sin\theta & 0 & \cos\theta \end{bmatrix}. \quad (4)$$

Besides, a rotation of angle ψ about the z-axis is defined as

$$\mathbf{R}_z(\psi) \triangleq \begin{bmatrix} \cos\psi & \sin\psi & 0 \\ -\sin\psi & \cos\psi & 0 \\ 0 & 0 & 1 \end{bmatrix} \quad (5)$$

where ψ , θ and ϕ can be called the Euler angles.

In the process of aerial refueling, the rotation between the receiver aircraft and the drogue is limited in a small range to ensure the safety, which can be ignored. So, assume that there is only translation which can be expressed as

$$\mathbf{p}_c = \mathbf{p}_d + \mathbf{t}_d^c. \quad (6)$$

Using (6), equations of position parameters can be established and solved.

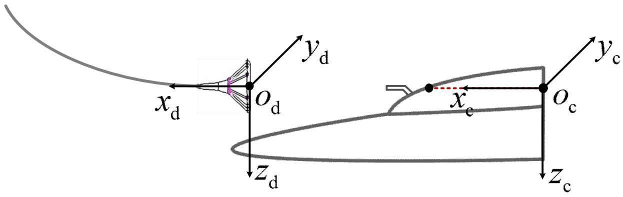

Figure 2. The coordinate system of the refueling system [16]

C. Camera Pinhole Model

Assume that a vector $\mathbf{p}_i \triangleq [u \; v]^T$ is in the image coordinate system $o_i - x_i y_i$. The camera pinhole model (see Fig. 3) is used to transform $\mathbf{p}_c$ and $\mathbf{p}_d$ to $\mathbf{p}_i$ as follows

$$s\begin{bmatrix} u \\ v \\ 1 \end{bmatrix} = \begin{bmatrix} \alpha_x & 0 & u_0 & 0 \\ 0 & \alpha_y & v_0 & 0 \\ 0 & 0 & 1 & 0 \end{bmatrix} \begin{bmatrix} x_c \\ y_c \\ z_c \\ 1 \end{bmatrix} = \mathbf{M} \begin{bmatrix} \mathbf{R}_d^c & \mathbf{t}_d^c \\ 0 & 1 \end{bmatrix} \begin{bmatrix} x_d \\ y_d \\ z_d \\ 1 \end{bmatrix}, \quad (7)$$

and

$$\mathbf{M} = \begin{bmatrix} \alpha_x & 0 & u_0 \\ 0 & \alpha_y & v_0 \\ 0 & 0 & 1 \end{bmatrix}, \quad (8)$$

where s in (7) is the scaling factor; $\mathbf{M}$ is the camera intrinsic matrix, in which α_x, α_y, u_0 and v_0 are determined by camera calibration [16].

D. Problem Formulation

According to the descriptions above, it is obtained that some markers are placed on the drogue. Let the number of the markers be N. As all markers are placed in the same plane, their depth information is identical, which can be expressed as s. Thus the markers in the image can be described as $(u_i, v_i, s), i = 1, 2, \cdots, N$. Since the markers compose a circle, it is necessary to obtain the center coordinate and radius of the circle, which can be expressed as (a, b, r). With these parameters, the relative distance between the drogue and the receiver aircraft is obtained. However, as the external environment is complicated and full of interferences, some essential measures should be taken, which can ensure the accuracy of the parameters and improve the robustness of the whole system.

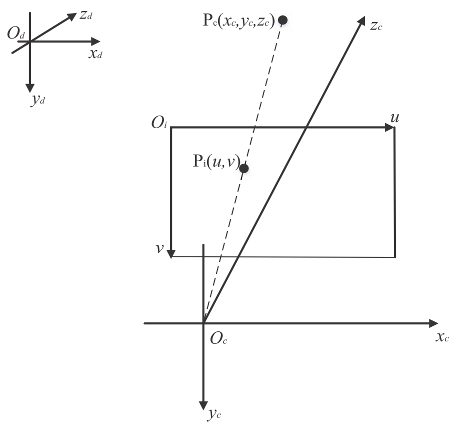

Figure 3. Camera pinhole model [17]

There are two major tasks in this paper: drogue recognition and enhancing detection robustness. Enhancing detection robustness is based on the prediction of the markers' coordinates, and it can be divided into three parts corresponding to different situations. Therefore, for simplicity, they are formulated into the following four steps.

- Assume that there is no disturbance and the whole refueling system works well. According to the known parameters $(u_i, v_i, s), i = 1, 2, \cdots, N$, get the the center and radius of the circle (a, b, r).
- According to the relative distance between the drogue and the receiver aircraft got before, estimate the coordinates of the markers in next moment and revise the current data.
- Assume that there are some noise and redundant points in the image. According to the known parameters $(u_i, v_i, s), i = 1, 2, \cdots, N$ and the equation of the circle, eliminate the influence of interferences.
- Assume that there are some markers undetectable. According to the current and predictive coordinates of the markers, bring forward corresponding measures.

Next, the main algorithm will be introduced in Section III in detail.

III. Main Algorithm for Position Estimation

A. Markers Detecting and Matching

As shown above, markers placed on the drogue are arranged as a circle. In the process of aerial refueling, the receiver aircraft should track the tanker aircraft with high accuracy. Thus, the angle of attack of the receiver aircraft is very small, according to which the drogue can be approximated to a circle. Its projection on the image can be expressed in the function form as

$$(x-a)^2 + (y-b)^2 = r^2 \tag{9}$$

where (a, b) denotes the center coordinate of the circle, r the radius of the circle. Let N be the number of all detected markers. And the detected markers can be expressed as $\mathbf{p}_i \triangleq [x_i \ y_i]^{\mathrm{T}}, i = 1, 2, \cdots, N$. To describe the difference between the observed value and the estimated value, here we use the residuals ε_i, which can be shown as

$$\varepsilon_i = (x_i - a)^2 + (y_i - b)^2 - r^2. \tag{10}$$

The cost function can be the sum of the residuals' square, that is

$$J = \sum_{i=1}^{N} \varepsilon_i^2 = \sum_{i=1}^{N} \left[(x_i - a)^2 + (y_i - b)^2 - r^2 \right]^2. \tag{11}$$

According to the principle of the least square, when the partial derivative of the cost function equals zero, the optimal fitting result is achieved. The result can be written in the numerical form as

$$\begin{cases} \dfrac{\partial J}{\partial a} = -4(x_i - a)\sum_{i=1}^{N}\left[(x_i - a)^2 + (y_i - b)^2 - r^2 \right] = 0 \\ \dfrac{\partial J}{\partial b} = -4(y_i - b)\sum_{i=1}^{N}\left[(x_i - a)^2 + (y_i - b)^2 - r^2 \right] = 0 \\ \dfrac{\partial J}{\partial r} = -4r\sum_{i=1}^{N}\left[(x_i - a)^2 + (y_i - b)^2 - r^2 \right] = 0. \end{cases} \tag{12}$$

With these functions, the parameters of the circle are obtained as

$$\begin{cases} a = \dfrac{(\overline{x^2}\cdot\bar{x} + \bar{x}\cdot\overline{y^2} - \overline{x^3} - \overline{xy^2})(\overline{y^2} - \bar{y}^2)}{2(\overline{x^2} - \bar{x}^2)(\overline{y^2} - \bar{y}^2) - 2(\bar{x}\cdot\bar{y} - \overline{xy})^2} - \\ \qquad \dfrac{(\overline{x^2}\cdot\bar{y} + \bar{y}\cdot\overline{y^2} - \overline{x^2y} - \overline{y^3})(\bar{x}\cdot\bar{y} - \overline{xy})}{2(\overline{x^2} - \bar{x}^2)(\overline{y^2} - \bar{y}^2) - 2(\bar{x}\cdot\bar{y} - \overline{xy})^2} \\ b = \dfrac{(\overline{x^2}\cdot\bar{y} + \bar{y}\cdot\overline{y^2} - \overline{x^2y} - \overline{y^3})(\overline{x^2} - \bar{x}^2)}{2(\overline{x^2} - \bar{x}^2)(\overline{y^2} - \bar{y}^2) - 2(\bar{x}\cdot\bar{y} - \overline{xy})^2} - \\ \qquad \dfrac{(\overline{x^2}\cdot\bar{x} + \bar{x}\cdot\overline{y^2} - \overline{x^3} - \overline{xy^2})(\bar{x}\cdot\bar{y} - \overline{xy})}{2(\overline{x^2} - \bar{x}^2)(\overline{y^2} - \bar{y}^2) - 2(\bar{x}\cdot\bar{y} - \overline{xy})^2} \\ r = \sqrt{a^2 - 2\bar{x}a + b^2 - 2\bar{y}b + \overline{x^2} + \overline{y^2}} \end{cases} \tag{13}$$

where $\bar{x}$ and $\bar{y}$ denote the average value of x or y, and $\overline{x^m y^n} = \dfrac{\sum_{i=1}^{N} x_i^m y_i^n}{N}, m, n \in [0, 3]$.

On the basis of camera pinhole model, the depth s of the plane at which the markers are located can be obtained by the radius of the circle. The function is as follows

$$\frac{R_{\mathrm{dr}}}{s+f} = \frac{r}{f} \tag{14}$$

where R_{dr} is the actual radius, f is the focal length of the camera. Let the coordinate of the probe in the image be $\mathbf{p}_{\mathrm{i}} \triangleq [u \ v]^{\mathrm{T}}$, and the distance between the probe and the camera in z-axis be d. The relative distance between the drogue and the probe can be expressed as

$$\begin{cases} \Delta x = |a-u| \cdot \dfrac{R_{\mathrm{dr}}}{r} \\ \Delta y = |b-v| \cdot \dfrac{R_{\mathrm{dr}}}{r} \\ \Delta z = \left| \dfrac{fR_{\mathrm{dr}}}{r} - f - d \right|. \end{cases} \tag{15}$$

Although the form of this algorithm is complex, its time complexity is just $O(n)$, which is suitable for computer implementation.

B. KF and Robust Image Tracking Algorithm

In this subsection, KF is applied to estimate the position of markers, which can reduce the influence of error points and improve the matching accuracy. The equations of state and measurement are given as follows

$$\mathbf{x}(k+1) = \mathbf{\Phi}(k+1,k)\mathbf{x}(k) + \mathbf{\Gamma}(k+1,k)\mathbf{W}(k) \tag{16}$$

$$\mathbf{z}(k) = \mathbf{H}(k)\mathbf{x}(k) + \mathbf{V}(k). \tag{17}$$

In above functions, $\mathbf{x}(k)$ is the 6×1 dimensional state vector of the system state, which is written as

$$\mathbf{x} = \begin{bmatrix} \Delta x & \Delta y & \Delta z & \Delta v_{\mathrm{x}} & \Delta v_{\mathrm{y}} & \Delta v_{\mathrm{z}} \end{bmatrix}^{\mathrm{T}} \tag{18}$$

where $\Delta x, \Delta y, \Delta z$ are the relative distances between the receiver aircraft and the drogue along three axes, respectively. And $\Delta v_{\mathrm{x}}, \Delta v_{\mathrm{y}}, \Delta v_{\mathrm{z}}$ are velocity differences; $\mathbf{z}(k)$ is the 3×1 dimensional observation vector, which is expressed as

$$\mathbf{z} = \begin{bmatrix} u & v & s \end{bmatrix}^{\mathrm{T}}. \tag{19}$$

And $\mathbf{H}(k)$ can be obtained from the correspondence of the image and the real world. Besides, other parameters can be expressed as

$$\mathbf{\Phi}(k+1,k) = \begin{bmatrix} \mathbf{0}_3 & \mathbf{I}_3 \\ \mathbf{0}_3 & \mathbf{0}_3 \end{bmatrix} \tag{20}$$

$$\mathbf{\Gamma}(k+1,k) = \begin{bmatrix} \mathbf{0}_3 \\ \mathbf{I}_3 \end{bmatrix}. \tag{21}$$

Given the initial value, the well-known KF consisting of prediction and estimation parts can start to iterate. The estimation of the states can be sent to the autopilot for the docking control. KF can also improve the system robust performance enormously which will ensure the normal operation of the whole refueling system.

C. The Dispose of Noise and Redundant Point

As the environment around the refueling equipment is complex, it is a common phenomenon that some noise and redundant points appear in the image, which may affects the matching of the drogue. These superfluous points may emerge for the following reasons: direct sunlight, light reflecting on he surface of the tanker aircraft, the noise points generated by the camera. The corresponding measures are given as follows.

For the drogue of the refueling system, let the center coordinate of estimation in world space $\mathbf{z} = [\Delta x \; \Delta y \; \Delta z]^{\mathrm{T}}$. According to the projection relation, the next center and radius of the circle in the image can be forecasted as (a,b) and r, and the estimation errors are $\Delta a, \Delta b, \Delta r$, respectively. For the image point (u,v) in the next moment, the judgment rules can be expressed as follows

$$\sqrt{(u_i-a)^2 + (v_i-b)^2} > \sqrt{\Delta a^2 + \Delta b^2} + r + \Delta r \tag{22}$$

or

$$\sqrt{(u_i-a)^2 + (v_i-b)^2} < r - \Delta r. \tag{23}$$

The two formulas have a similar effect, which can distinguish the unwanted points with high efficiency. If the point satisfies the condition (22) or (23), it will be removed.

In addition, as the markers located on the drogue are placed as a circle, let the current circle in the image be (a,b,r). If the error of fitting is greater than the threshold value ε set earlier, this point should be removed. The function can be expressed as

$$\frac{(u_i-a)^2 + (v_i-b)^2 - r^2}{r} > \varepsilon. \tag{24}$$

In actual operation, the value of ε can be got from real experiments.

The first algorithm shown above removes the unsuitable points in the aspect of the markers' movement tendency, while the other does the same in the aspect of markers' geometry distribution property. Together with other necessary logical judgments, most errors can be discovered and got rid of, which can ensure the accuracy of position estimation.

D. The Algorithm of Losing Points

When the probe-and-drogue refueling system is operating, there is a common phenomenon that some of the markers may be out of the camera's view or obscured by the probe or other obstacles. Due to the determination of parameters of the circle (a,b,r), three detectable markers should be prepared at least. By estimating the coordinates of the markers in the image, whether or not there are markers out of sight can be determined in advance. Different states and necessary countermeasures are listed as follows.

State 1: If some of the markers are out of sight, and other visible markers are near the probe, this situation says that the invisible markers are obscured by the probe. If they are just out of sight for a short time, which is less than the threshold value t_{i}, the estimation results of KF can fill the missing directly, which can maintain system operation. However at the same time, an alarm is provided until all return to normal.

State 2: If some markers are blocked by the probe for such a long time, as exceeds the threshold value t_{i}, it is necessary to check the number of markers available. If the number is less than three, it is illustrated that the position estimation system is in bad condition, which may lead to huge safety risks. So the receiver aircraft should stop refueling process immediately. Until the receiver aircraft returns to a safe place, a next refueling attempt is not allowed to begin.

State 3: If some markers are out of sight, and the existing markers are near the four boundaries of the camera's view, it shows that the invisible markers are beyond the camera's view. If this situation occurs, it implies that there is something wrong with the relative position between the receiver aircraft and the tanker aircraft. If all the missing markers return to view after a short period, which is less than the threshold value t_p, the refueling process can be permitted to carry on. If not, the refueling process must be stopped at once. An alarm is also required in this process.

The threshold values t_i and t_p can be got from real experiments. However according to the intensity of the event, t_p is much smaller than t_i. With these countermeasures, the robustness of the whole refueling system can be highly improved.

IV. SIMULATION AND RESULTS

A. Simulation Environment

To observe the simulation results intuitively, a 3D simulation model is created by the virtual reality toolbox of Matlab, which emulates the process of aerial refueling precisely. The interface of this model is shown as follows (see Fig. 4).

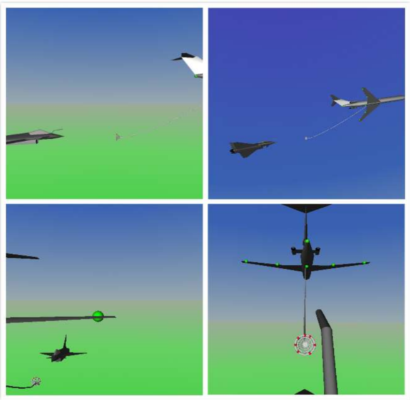

Figure 4. Aerial refueling of VR simulation

The coordinate system of the virtual camera in this simulation model is different from the one in Section II. Its origin is the current location set by the user, with x_c axis pointing forward, y_c pointing upward, z_c pointing right. In addition, the pixel resolution of the virtual camera is 860 pixels × 480 pixels. Moreover, its maximum frame rate is 50 frames per second. What is more, its angle of view is 90 degrees.

In order to test the effectiveness and practicability of the vision-based algorithm proposed in Section III, let the drogue stay still in a series of simulations, and at the same time, the receiver aircraft is moved along the trajectory set in advance, for example, sinusoidal movement in three axes. According to the image acquired by the virtual camera on the receiver aircraft, the relative distance between the receiver aircraft and the drogue can be solved.

B. Marker Identification

For the convenience of establishing the model, some colored spheres substitute for the passive reflectors which are attached to the drogue and the tanker aircraft. The color of the spheres on the drogue is set to be red, while green on the tanker aircraft. The two kinds of spheres are distinguished by color, and then treated differently.

In the image obtained by the virtual camera, the markers appear to be bright. Thus, image gray processing (25) and thresholding function (26) are sufficient to detect markers. Then erode the bright pixel blob to eliminate noise according to the threshold value w. Finally, the center coordinates of the pixel blob can be obtained, that is, pixel coordinates of the markers.

$$\mathbf{Gray}(u,v) = 2\mathbf{R}(u,v) - \mathbf{G}(u,v) - \mathbf{B}(u,v) \tag{25}$$

$$\mathbf{Gray}(u,v) = \begin{cases} 255, \textit{ if } \mathbf{Gray}(u,v) \geq w \\ 0, \textit{ otherwise} \end{cases}. \tag{26}$$

C. Simulation Results

The whole simulation lasts for 200 seconds, while real-time pictures are displayed in two windows. The images of different situations are listed as follows (see Fig. 5 6)

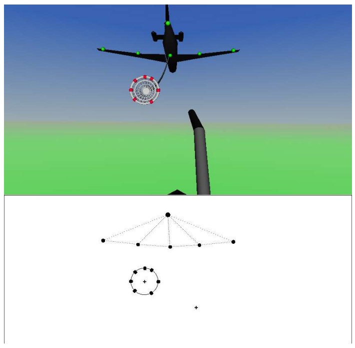

Figure 5. All markers are identified properly

From these figures, it is obtained that the circle matching algorithm can work well even if some markers are blocked or beyond the boundary. Besides, even though the external environment is complex, the system can ensure a high-precision position estimation. These conclusions show the high robustness of this position estimation system. The positioning data and actual data are compared as follows (see Fig. 7)

In Fig. 7, the dotted line represents the relative distance solved by vision-based position estimation algorithm, while the solid line represents the real distance. Besides, in Fig. 8, the tracking error of three axes is obtained. It can be obtained that the system can get better localization information of the drogue.

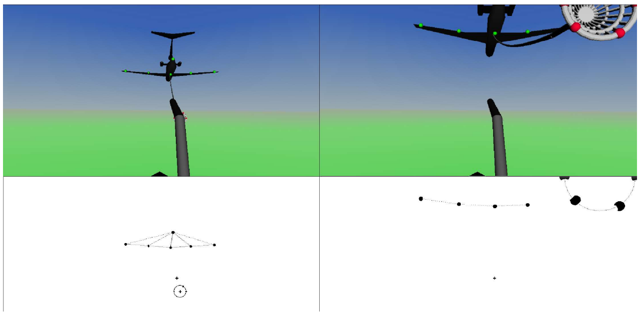

Figure 6. 50% and 85% of the drogue is blocked.

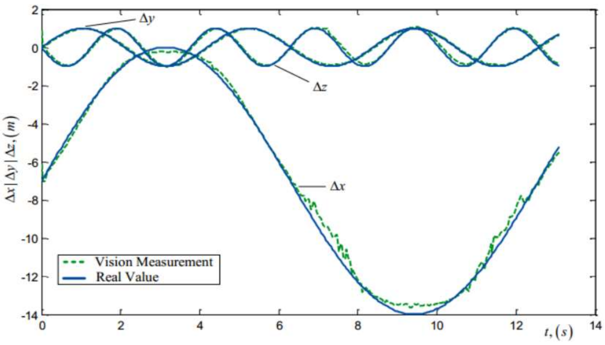

Figure 7. The effect of visual location and tracking.

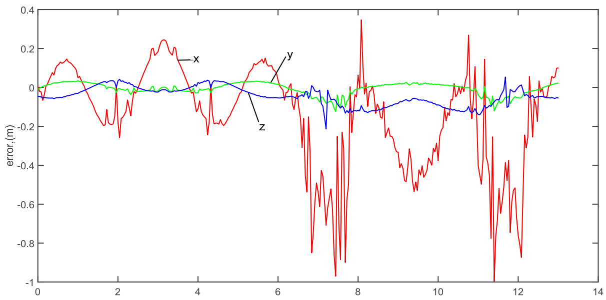

Figure 8. The tracking error of three axes.

V. CONCLUSION

In this research, a vision-based position estimation method for probe-and-drogue refueling system is presented. These real-time detecting and matching algorithms are of strong robustness. Through the simulation, the effectiveness and accuracy of the proposed method have been demonstrated. Therefore, the proposed vision-based position estimation method is promising to acquire the relative distance information between the drogue and the receiver aircraft, which can be later applied to the autonomous aerial refueling system.

The future work is to test the proposed method with a real camera, such as in a hardware-in-the-loop simulation. Besides, some other extreme circumstances which may happen in real flight should be considered.

ACKNOWLEDGMENT

The financial supports from the National Natural Science Foundation of China (61473012) for this work are greatly acknowledged.

REFERENCES

[1] C. Bolkcom, “Air force aerial refueling methods: flying boom versus hose-and-drogue”, *Congressional Research Service, The Library of Congress*, June 2006, Order Code RL32910.

[2] J. P. Nalepka and J. L. Hinchman, “Automated aerial refueling: extending the effectiveness of unmanned air vehicles”, *AIAA Modeling and Simulation Technologies Conference and Exhibit*, 2005, AIAA 2005-6005.

[3] G. Campa, M. Mammarella, M. R. Napolitano, et al, “A comparison of pose estimation algorithms for machine vision based aerial refueling for UAVs”, *Proceedings of the 2006 Conference on Control and Automation, Mediterranean*, 2006:1-6

[4] S. M. Ross, M. D. Menza and E. T. Waddell, “Demonstration of a control algorithm for autonomous aerial refueling (Project “No Gyro”)”, *Technical report, Air Force Flight Test Center Edwards AFB CA*, 2005.

[5] J. L. Hansen, J. E. Murray and N. V. Campos, “The NASA Dryden AAR Project: A flight test approach to an aerial refueling system”, *AIAA Atmospheric Flight Mechanics Conference and Exhibit*, 2004, AIAA 2004-4939.

[6] W. R. Williamson, G. J. Glenn, V. T. Dang, et al, “Sensor fusion applied to autonomous aerial refueling”, *Journal of Guidance, Control and Dynamics*, 2009, 32(1):262-275.

[7] J. N. Fu, Q. Fu, U. Arif, Q. Quan, “A pose estimation method of a moving target based on off-board monocular vision”, *Guidance, Navigation and Control Conference (CGNCC), 2016 IEEE Chinese. IEEE*, 2017:2082-2087.

[8] J. Kimmett, J. Valasek and J. Junkins, “Autonomous aerial refueling utilizing a vision based navigation system”, *AIAA Guidance, Navigation and Control Conference and Exhibit*, 2002, AIAA 2002-4669.

[9] A. D. Weaver, “Using predictive rendering as a vision-aided technique for autonomous aerial refueling”, *M.S. Thesis, Air Force Institute of Technology*, 2009.

[10] Q. Fu, Q. Quan and K. Y. Cai, “Robust pose estimation for multirotor UAVs using off-board monocular vision”, *IEEE Transactions on Industrial Electronics*, 2017, 64(10): 7942-7951.

[11] S. Chen, H. B. Duan, Y. Deng, C. Li, G. Z. Zhao, Y. Xu, “Drogue pose estimation for unmanned aerial vehicle autonomous aerial refueling system based on infrared vision sensor”, *Optical Engineering*, 2017, 56(12): 124105.

[12] J. Valasek, K. Gunnam, J. Kimmett, et al, “Vision-based sensor and navigation system for autonomous air refueling”, *Journal of Guidance, Control and Dynamics*, 2005, 28(5):979-989.

[13] D. Monish, Tandale, R. Bowers and J. Valasek, “Trajectory tracking controller for vision based probe and drogue autonomous aerial refueling”, *Journal of Guidance, Control and Dynamics*, 2006, 29(4): 846-857.

[14] C. P. Lu, G. D. Hager and E. Mjolsness, “Fast and globally convergent pose estimation from video images”, *IEEE Transactions on Pattern Analysis and Machine Intelligence*, 2000, 22(6): 610-622.

[15] Q. Quan, “Introduction to multicopter design and control”, *Springer*, Singapore, 2017.

[16] Z. B. Wei, X. H. Dai, Q. Quan, K. Y. Cai, “Drogue dynamic model under bow wave effect in probe and drogue aerial refueling”, *IEEE Transactions on Aerospace and Electronic Systems*, 2016, 52(4): 1728-1742.

[17] P. Sturm, “Pinhole camera model”, *Springer*, Boston, 2014.